

Anti-oxidation characteristics of Cr-coating on surface of Ti-45Al-8.5Nb alloy by plasma surface metallurgy technique

Bing Zhou(周兵), Ya-Rong Wang(王亚榕), Ke Zheng(郑可), Yong Ma(马永), Yong-Sheng Wang(王永胜)†, Sheng-Wang Yu(于盛旺), and Yu-Cheng Wu(吴玉程)

Citation: Chin. Phys. B, 2020, 29 (**12**): 126101. DOI: 10.1088/1674-1056/aba9c2
Journal homepage: http://cpb.iphy.ac.cn; http://iopscience.iop.org/cpb

What follows is a list of articles you may be interested in

Structure and tribological properties of Si/a-C:H(Ag) multilayer film in stimulated body fluid

Yan-Xia Wu(吴艳霞), Yun-Lin Liu(刘云琳), Ying Liu(刘颖), Bing Zhou(周兵), Hong-Jun Hei(黑鸿君), Yong Ma(马永), Sheng-Wang Yu(于盛旺), and Yu-Cheng Wu(吴玉程)

Chin. Phys. B, 2020, 29 (**11**): 116101. DOI: 10.1088/1674-1056/ab9c10

Discovery of superhard materials via CALYPSO methodology

Shuangshuang Zhang(张爽爽), Julong He(何巨龙), Zhisheng Zhao(赵智胜), Dongli Yu(于栋利), Yongjun Tian(田永君)

Chin. Phys. B, 2019, 28 (**10**): 106104. DOI: 10.1088/1674-1056/ab4179

Enhancement of MAD/MIR phasing at low resolution and a new procedure for automatic phase extension

Pu Han(韩普), Yuan-Xin Gu(古元新), Wei Ding(丁玮), Hai-Fu Fan(范海福)

Chin. Phys. B, 2019, 28 (**7**): 076108. DOI: 10.1088/1674-1056/28/7/076108

Quantum density functional theory studies of structural, elastic, and opto-electronic properties of $ZMoO_3$ (Z=Ba and Sr) under pressure

Saad Tariq, A A Mubarak, Saher Saad, M Imran Jamil, S M Sohail Gilani

Chin. Phys. B, 2019, 28 (**6**): 066101. DOI: 10.1088/1674-1056/28/6/066101

Light trapping and optical absorption enhancement in vertical semiconductor Si/SiO_2 nanowire arrays

Ying Wang(王莹), Xin-Hua Li(李新化)

Chin. Phys. B, 2018, 27 (**2**): 026102. DOI: 10.1088/1674-1056/27/2/026102

Anti-oxidation characteristics of Cr-coating on surface of Ti-45Al-8.5Nb alloy by plasma surface metallurgy technique*

Bing Zhou(周兵), Ya-Rong Wang(王亚榕), Ke Zheng(郑可), Yong Ma(马永), Yong-Sheng Wang(王永胜)†, Sheng-Wang Yu(于盛旺), and Yu-Cheng Wu(吴玉程)

Institute of New Carbon Materials, Taiyuan University of Technology, Taiyuan 030024, *China*

(Received 28 May 2020; revised manuscript received 20 July 2020; accepted manuscript online 28 July 2020)

TiAl-based alloys have received extensive attention recently due to their excellent properties. However, the weak oxidation resistance at temperatures higher than 800 °C can limit their further high-temperature structural applications. To improve the oxidation resistance of a high-Nb-content γ-TiAl alloy (Ti-45Al-8.5Nb, in units of at.%), a chromium (Cr) coating is prepared by using the plasma surface alloying technique, separately, at 800 °C and 1000 °C. The x-ray diffraction (XRD) patterns reveal that an oxide surface layer consisting of Cr_2O_3, Al_2O_3, and TiO_2 is produced on the Cr-coated Nb containing γ-TiAl substrates during the initial oxidation. However, the Cr_2O_3 is dominated in the oxide surface layer after being isothermally oxidized for 300 h. The oxidation kinetic curves are composed of a parabolic law stage ($\leq$ 90 h) and a biquadratic law stage ($\geq$ 90 h), fit by weight–gain curves. Due to diffusion in the fabrication process and oxidation process, the Cr-coated specimens have an adhesion force after being isothermally oxidized, specifically 69 N for a specimen after oxidation for 300 h. These results demonstrate that the Cr coating enhances the oxidation resistance and adhesion of a Ti-45Al-8.5Nb alloy, which may provide a new feasible scheme for designing oxidation protection layers.

Keywords: titanium aluminum alloy, coating, isothermal oxidation, plasma surface alloying technique

PACS: 61.05.–a, 61.82.Bg, 68.37.–d **DOI:** 10.1088/1674-1056/aba9c2

1. Introduction

TiAl-based intermetallics, as high-temperature structural materials, are one of the most promising groups of candidates due to their low densities, high specific strengths, and excellent creep resistances, which all have great potential applications in aerospace and automotive industry.[1,2] However, the oxidation resistances of these alloys above 800 °C are weakened rapidly by forming a surface oxide layer consisting of porous TiO_2 and Al_2O_3.[2–5] As such, immense efforts have been made to improve the oxidation resistances of TiAl alloys to satisfy the requirements for engineering applications above 800 °C.

Numerous coatings, including ceramic coatings,[6–8] metallic coatings,[9,10] multi-component alloyed coatings,[11–13] and composite coatings,[14–16] have been prepared on the surfaces of TiAl alloys to improve their oxidation resistances. With respect to the fabrication methods, the sol–gel method,[6] powder packing[8] or multi arc ion plating,[9] and magnetron sputtering[15] have been extensively employed to fabricate the coatings. However, the difference in thermal expansion coefficient between the coatings and TiAl alloys results in holes and/or cracks, lowering the adhesion strength.[1,5] Moreover, the interdiffusion between elements of the coating and substrate worsens the adhesion due to the forming of new brittle phases and/or Kirkendall voids.[2,13] Therefore, it is necessary to develop techniques to obtain the coating with a stable composition, good adhesion and low residual stress.

The plasma surface alloying technology (PSAT) can effectively improve the surface properties of substrates through the metallurgical bonding pattern.[17,18] Usually, when the target material is bombarded and sputtered off by glow discharge of Ar ion, and then transported to the surface of substrate. At the same time, the substrate is heated by the electrons' bombardment to a high temperature. So, the target element deposited on the surface of substrate, forms a deposited layer. Moreover, the sub-surface forms a diffusion layer due to the thermal-driven diffusion between the deposited layer and substrate. Therefore, it has been employed for various alloys to ameliorate their surface properties,[19–21] including hardness, tribological properties, oxidation, or corrosion resistance. Due to the excellent oxidation resistance and melting salt corrosion resistance of ceramic Cr_2O_3, Cr coatings have been prepared on the surface of Ti-6Al-4V substrates by using PSAT, improving the oxidation and cyclic oxidation resistance of Ti-6Al-4V alloys.[22,23] Moreover, it was found that the Cr/CrC multilayer prepared on a γ-TiAl alloy substrate by the PAST not only improve the oxidation resistance (830 °C for 100 h) but also ameliorate the friction properties (friction coefficient of

*Project supported by the National Natural Science Foundation of China (Grant No. 51601122), the 2019–2020 Intergovernmental Cooperation Projects in Science and Technology of the Ministry of Science and Technology, China (Grant No. CB02-03), the Science and Technology Major Project of Shanxi Province, China (Grant No. 20181102013), the "331 Project" Engineering Research Center of Shanxi Province, China (Grant No. PT201801), the China Postdoctoral Science Foundation (Grant No. 2017M620574), and the Fund from the State Key Laboratory of Advanced Metal Materials, China (Grant No. 2019-ZD02).

†Corresponding author. E-mail: wangyongsheng@tyut.edu.cn

© 2020 Chinese Physical Society and IOP Publishing Ltd

$\sim$ 0.2).[24] However, many issues have not been clarified yet for such alloys, such as the composition diffusion, adhesion and anti-oxidation performance. Thus, in this work, Cr coatings are fabricated on a γ-typed Ti-45Al-8.5Nb alloy by using the PSAT. The oxidation resistance is evaluated in isothermal oxidation experiments at 900 °C for 90 h and 300 h in air. The composition, microstructure and adhesion properties are also investigated.

2. Experimental methods

TiAl alloy with a nominal composition of Ti-45Al-8.5Nb-(W, B, Y) in units of at.% was employed as a substrate in each experiment. All of the samples were cut into cuboid shapes each with a dimension of 10 mm×10 mm×5 mm by wire electrical discharge machining and ground by SiC sandpaper from 400 grits to 2000 grits. The Cr coatings were prepared on these Ti-45Al-8.5Nb substrates by PAST at 800 °C and 1000 °C with Cr plate and high-purity argon (99.99%), which were termed Cr/Substrate (800 °C) and Cr/Substrate (1000 °C) and denoted as Cr/S (800 °C) and Cr/S (1000 °C), respectively.[17,18] The morphology, composition, and microstructure of Cr coatings were then characterized by scanning electron microscopy (SEM, TESCAN MIRA3, Japan), energy-dispersive x-ray spectroscopy (EDS) and x-ray diffraction (XRD, UltimalV, Topvendor Technology, Japan). The initial and isothermal oxidation (Oxid.) tests including uncoated and Cr-coated Ti-45Al-8.5Nb substrates were carried out at 900 °C for 1 h, 3 h, 5 h, 90 h, and 300 h in a muffle-type furnace (SR2X, Kewei, China). All of the samples were placed into a quartz tube and weighed every 10 h for isothermal oxidation. An electrical balance with an accuracy of 0.0001 g (ME104E, Mettler Toledo, Switzerland) was employed to record the quality changes of all samples. All of the oxidized samples were characterized by using SEM, EDS, and XRD to determine their morphologies, compositions, and microstructures. The adhesion force was tested by using a scratch test (HT-5001, Huijin Tier Plating Technology, China) with a load ranging from 5 N to 160 N. The loading speed was 80 N/min and the scratch speed was 2 mm/min.

3. Results

3.1. Characterization of Cr coatings

Figure 1 shows the surface and cross-sectional morphologies, as well as EDS line-scan profiles of the Cr coatings fabricated at 800 °C and 1000 °C. The island-like Cr particles cover the whole surface of substrate as shown in Figs. 1(a) and 1(d) (their insets). The composition of the coating surface is Cr element with content of 98.1%, which is identified by mapping analysis (Table 1). The deposited Cr layer and the interfusion layer constitutes a Cr coating [see Fig. 1(b)]. The thickness of the deposited Cr layer is $\sim$3.2 μm for the specimen fabricated at 800 °C, but increases to $\sim$ 5.1 μm for the specimen prepared at 1000 °C [see Fig. 1(e)]. Both samples are free from pores or cracks between the deposited Cr layer and the TiAl substrate.

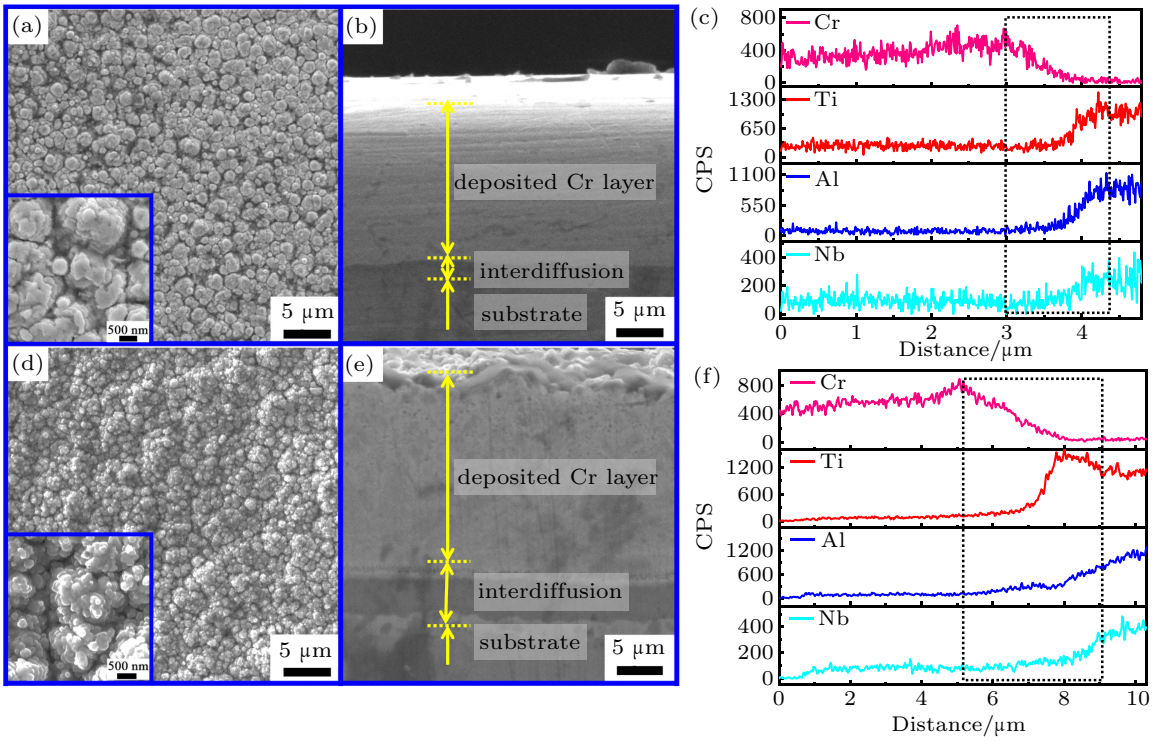


Fig. 1. (a) Surface and (b) cross-sectional morphology at 800 °C, and (c) EDS line-scan profile marked in panel (b); (d) surface and (e) cross-sectional morphology at 1000 °C and (f) EDS line-scan profile marked in panel (e).

The elemental distribution and diffusion between these layers are characterized by EDS of line scan [see Figs. 1(c) and 1(f)]. The thickness of diffusion layer of Cr element, formed between the deposited Cr layer and the substrate at a fabrication temperature of 800 °C, is ∼ 1 μm, but it is ∼ 3 μm at a fabrication temperature of 1000 °C. Moreover, the main elements such as the aluminum, titanium and niobium element of the substrate also diffused toward the Cr layer. The interdiffusion zone caused by varying the content of different elements plays a key role in the transition and bonding between the Cr coating and the substrate.[18,25]

3.2. Initial oxidation

Figure 2 displays the surface morphologies of Cr-coated specimens (fabricated at 1000 °C) after an initial oxidation at 900 °C. After being oxidized for 1 h, fine oxide particles form on the surface [see Figs. 2(a) and 2(d)]. Moreover, the oxygen content increases to 67.3% (Table 1). As the oxidation time increases to 3 h, the oxide particles further assemble, leading to a coarser surface [see Figs. 2(b) and 2(e)]. When the oxidation time increases to 5 h, the oxide particles distribute more and more uniformly to form a denser surface [see Figs. 2(c) and 2(f)]. Also, the content of oxygen is 51.9%.

Figure 3 shows the XRD results of the coating surface from all specimens. Due to the existence of deposited and diffusion layers (Fig. 1), the Cr-coated specimen before oxidation is comprised of Cr, TiAl, Ti_3Al, Cr_2Ti, and $AlCr_2$ phase identified by XRD patterns. The deposited Cr layer is on the top surface, while the AlCr phase is in the diffusion layer, Ti_3Al and TiAl belongs to the substrate, which is determined by combined analyses of XRD and SEM results. After being oxidized for 1 h, a Cr_2Ti phase at 63.46° obviously disappears, but new phases including Cr_2O_3 [at 35.88°, 44.31°, and 65.24° corresponding to (110), (202), and (300)], TiO_2 [at 27.32°, 53.98°, 62.41°, and 68.60°] and Al_2O_3 [at 31.60°, 38.71°, 45.23°, and 50.69°] form simultaneously besides the deposited Cr layer and the Ti_3Al and TiAl of the substrate. A possible reason is that the Cr_2O_3 does not form a continuous film to cover the whole surface in a short time because not all Cr atoms on the surface are oxidized to form Cr_2O_3, and thus leading the oxygen ions to diffuse inward, generating Al_2O_3 and TiO_2. With the increase of oxidation time, the Cr_2O_3 peaks instead of the Al_2O_3 and TiO_2 peaks become more pronounced.

Table 1. Chemical compositions of Cr/substrate in Figs. 1 and 2, analyzed by EDS (in unit at.%).

Samples	Cr/S (1000 °C) Oxid. 0 h	Cr/S (1000 °C) Oxid. 1 h	Cr/S (1000 °C) Oxid. 3 h	Cr/S (1000 °C) Oxid. 5 h
O Kal	–	67.3	66.1	51.7
Cr Kal	98.1	24.4	33.3	47.2
Al Kal	1.2	8.2	–	–
Ti Kal	0.7	0.1	0.6	1.1
Nb Kal	–	–	–	–

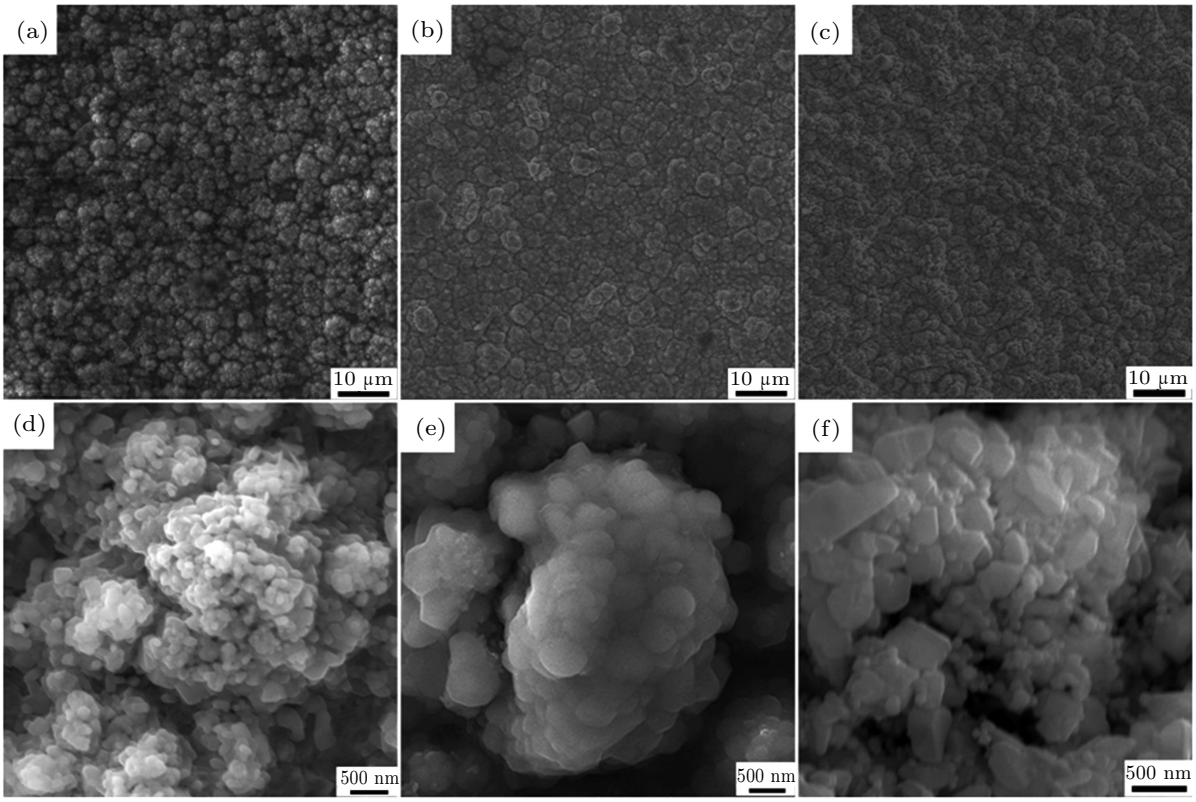


Fig. 2. SEM images of Cr/substrate fabricated at 1000 °C after initial oxidation time of [(a) and (d)] 1 h, [(b) and (e)] 3 h, and [(c) and (f)] 5 h.

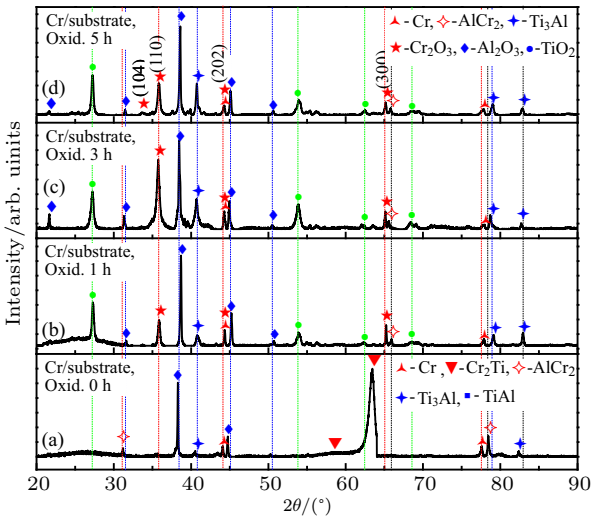


Fig. 3. XRD patterns of Cr/substrates oxidized for (a) 0 h, (b) 1 h, (c) 3 h, and (d) 5 h.

3.3. Isothermal oxidation behaviors

Figure 4 shows the oxidation kinetic curves of the uncoated and Cr-coated TiAl alloys after being oxidized for 90 h and 300 h. When the oxidation time is within ∼ 90 h, the oxidation weight rate increases quickly for the uncoated and coated specimens, reaching 0.9 mg/cm^2 after being oxidized for ∼ 90 h [Fig. 4(a)]. However, the oxidation growth rate of the uncoated alloy is accelerated continuously and reaches 1.97 mg/cm^2 after being oxidized for 300 h, [Fig. 4(b)]. By comparison, the mass gained of Cr/substrate (800 °C) and Cr/substrate (1000 °C) specimens increase with a low growth rate of ∼ 1.06 mg/cm^2 and ∼ 1.10 mg/cm^2 after being oxidized for 300 h, respectively. This result indicates that a protective oxide film on the Ti-45Al-8.5Nb alloy forms to prevent oxygen in air from diffusing into the substrate.

Figure 5 shows the XRD results of the uncoated and Cr-coated substrates after being isothermally oxidized at 900 °C. An oxide film including Al_2O_3 and TiO_2 forms on the surface of the uncoated substrate after being oxidized for 300 h. Peaks of $AlNb_2$ are also detected by the XRD because of the very thin oxide film, similar to the previous reports.[5,26] The oxide film of coated substrate mainly consists of Cr_2O_3, Al_2O_3, and TiO_2 after being oxidized for 90 h. For the initial oxidation (Fig. 3), the Cr_2O_3 peaks become stronger than those of Al_2O_3 and TiO_2, and more new peaks of Cr_2O_3 and Al_2O_3 are formed after being oxidized for 90 h. However, the Cr_2O_3 is the main phase instead of Al_2O_3 in the Cr-coated substrate after being oxidized for 300 h. A possible reason is that the more and more Cr elements are oxidized to form a Cr_2O_3 film, thereby increasing the thickness of Cr_2O_3 film formed and reducing the amount of oxygen diffusing into the coating and the substrate.

The surface micrographs of Cr-coated specimens exposed to the air, isothermally oxidized at 900 °C for 90 h and 300 h, are shown in Figs. 6(a)–6(d). The Cr_2O_3 particles in the film after being oxidized for 300 h become larger in size and more densely stacked than those in the case with oxidation time of 90 h. The dense Cr_2O_3 film effectively prevents oxygen in the ambient air from entering into the film, and thus resulting in the low rate of oxidation. This is consistent with the oxidation kinetics curve in Fig. 5. The cross-sections of coated specimens are characterized by SEM [Figs. 6(a1)–6(d1)] and EDS [Figs. 6(a2)–6(d2)]. The oxide films of the Cr-coated specimens after being oxidized for 90 h each consist of an outermost layer of Cr_2O_3, and mixed layers including Cr_2O_3, Al_2O_3, and TiO_2 (Table 2).

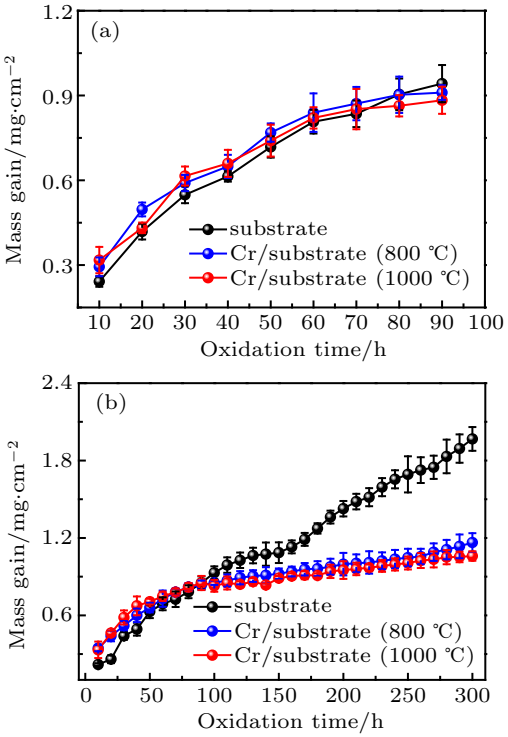


Fig. 4. Isothermal oxidation kinetic curves for substrate and Cr coatings fabricated at 800 °C and 1000 °C and oxidized for (a) 90 h and (b) 300 h.

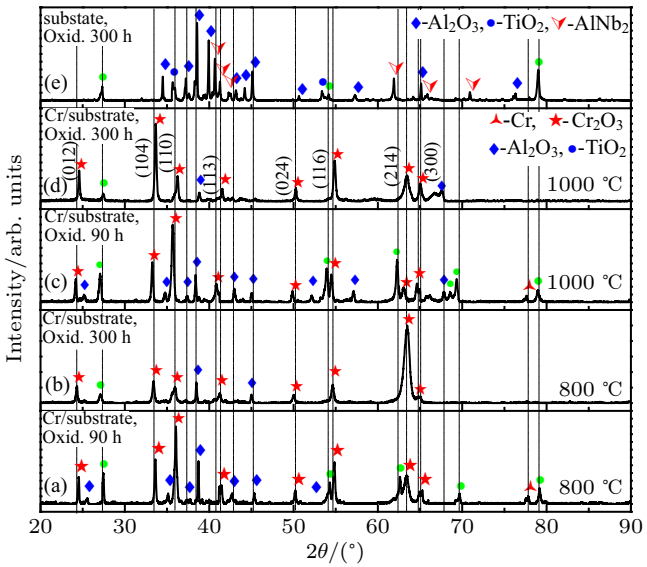


Fig. 5. XRD patterns of [(a) and (b)] Cr/substrate fabricated at 800 °C and oxidized for 90 h and 300 h, respectively; [(c) and (d)] Cr/substrate fabricated at 1000 °C and oxidized for 90 h and 300 h, respectively; (e) substrate oxidized for 300 h.

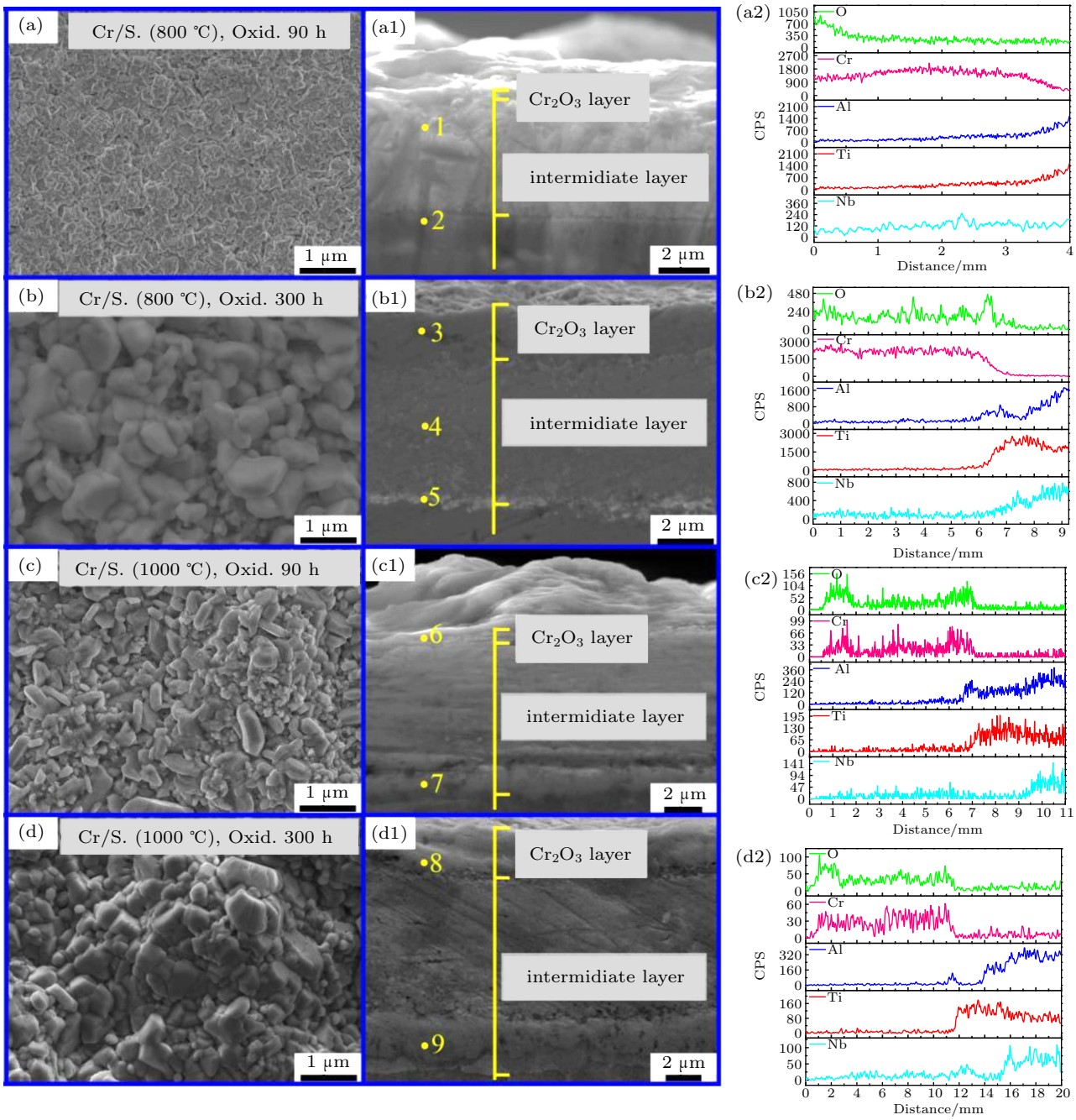


Fig. 6. Morphology of (a) surface and (a1) cross sectional for Cr/substrate (Cr/S.) fabricated at 800 °C and oxidized for 90 h, and (a2) EDS line-scan profile marked in panel (a1). (b) Morphology of surface and (b1) Cr/substrate fabricated at 800 °C and oxidized for 300 h, and (b2) EDS line-scan profile marked in panel (b1). (c) Morphology of surface and (c1) cross-sectional for Cr/substrate fabricated at 1000 °C and oxidized for 90 h, and (c2) EDS line-scan profile marked in panel (c1). (d) Morphology of surface and (d1) Cr/substrate fabricated at 1000 °C and oxidized for 300 h, and (d2) EDS line-scan profile marked in panel (d1).

Table 2. Chemical compositions of Cr/substrate in Figs. 6(a)–6(d), analyzed by EDS (in unit at.%).

Sample	Substrate Oxid. 90 h	Substrate Oxid. 300 h	Cr/S. (800 °C) Oxid. 90 h	Cr/S. (800 °C) Oxid. 300 h	Cr/S. (1000 °C) Oxid. 90 h	Cr/S. (1000 °C) Oxid. 300 h
O Kal	61.8	65.2	53.9	61.5	57.3	58.15
Cr Kal	–	–	43.4	37.2	41.3	32.63
Al Kal	28.4	14.2	0.7	0.2	1.2	7.1
Ti Kal	9.2	14	2.0	1.0	0.2	2.12
Nb Kal	0.4	6.6	–	0.1	–	–

A corresponding mapping results of the Cr-coated specimens can be found in Fig. 7. A bright boundary between the oxide film of oxygen and Cr elements and the substrate of the aluminum, titanium, and niobium elements indicates the strong oxidation resistance of Cr_2O_3 film. Comparing with Figs. 1(c) and 1(f), the Cr element within the coating and the aluminum, titanium, and

niobium elements of the substrate diffuse slightly toward each other [Figs. 6(c2) and 7(e)–7(e5)] after being oxidized for 90 h. Moreover, the pure Cr element still exists in the coating due to preventing oxygen from entering into the Cr_2O_3 film, which can be seen from the XRD patterns and Table 3. By comparison, the obvious interdiffusion of Cr is caused by the longer oxidation time for the Cr-coated specimen oxidized for 300 h [Figs. 6(d2) and 7(f)–7(f5)]. The Cr_2O_3 film becomes thicker due to the formation of more Cr_2O_3.

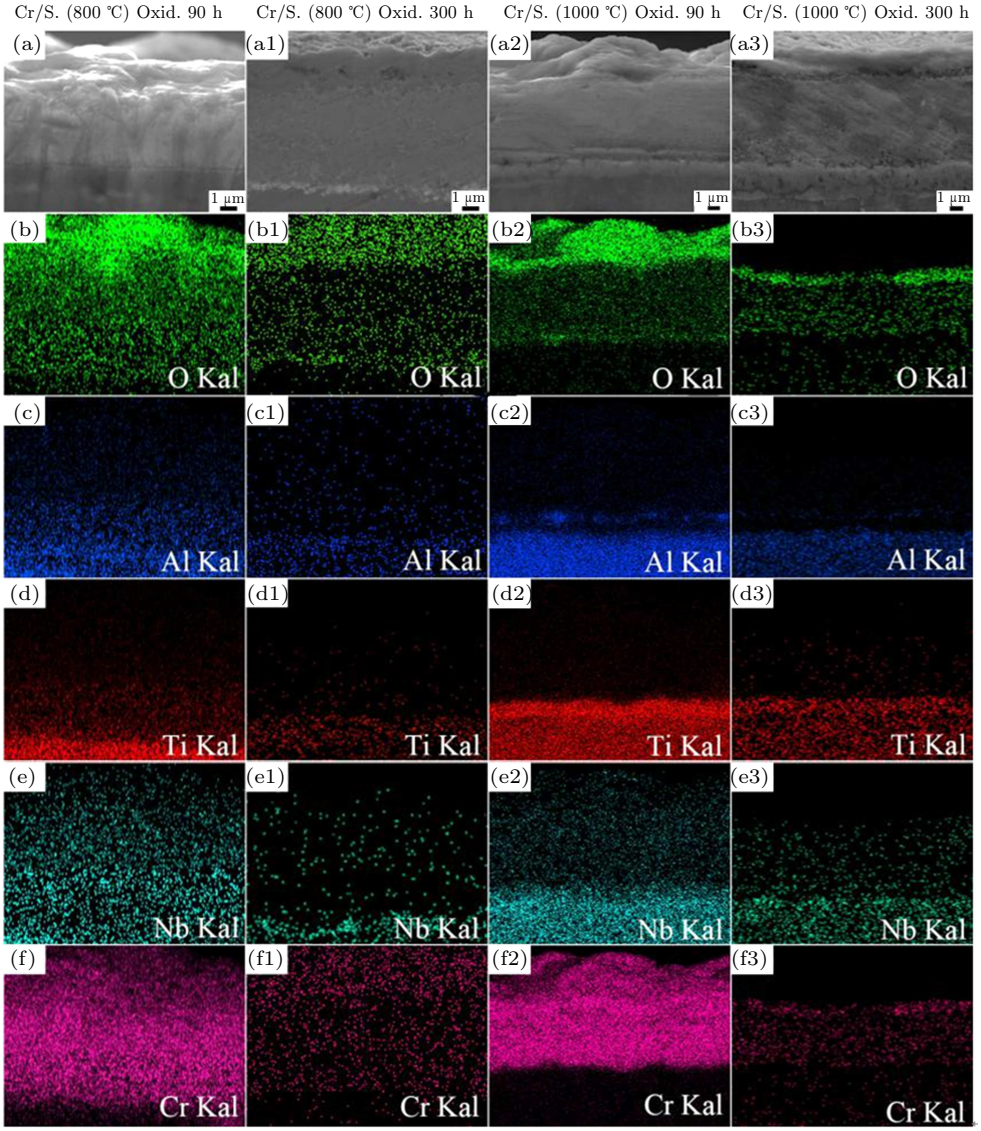


Fig. 7. Morphology of (a) cross section of Cr/substrate fabricated at 800 °C and oxidized for 90 h, and [(a2)–(a5)] EDS map-scan profiles. Morphology of (b) cross section of Cr/substrate fabricated at 800 °C and oxidized for 300 h, and [(b2)–(b5)] EDS map-scan profiles. Morphology of (c) cross sectional of Cr/substrate fabricated at 1000 °C and oxidized for 90 h, and [(c2)–(c5)] EDS map-scan profiles. Morphology of (d) cross sectional of Cr/substrate fabricated at 1000 °C and oxidized for 300 h, and [(d2)–(d5)] EDS map-scan profiles.

Table 3. Chemical compositions of Cr/substrate in Figs. 6(a1)–6(d1), analyzed by EDS (in unit at.%).

Elements	O Kal	Cr Kal	Al Kal	T Kal	Nb Kal
1	21.7	49	12.1	17.2	–
2	15.6	–	40.6	33.8	9.6
3	65.8	33.2	0.5	0.5	–
4	51.7	43.5	2.5	2.3	–
5	52.5	0.7	29.7	16.1	0.9
6	10	88.2	0.3	1.5	–
7	49.1	4	7.3	37.2	2.4
8	24.1	75.9	–	–	–
9	19.8	–	–	76.1	4.1

3.4. Adhesion property

The adhesion force of uncoated and Cr-coated substrates are investigated by using a scratch test as shown Fig. 8. A sharp peak caused by the remarkable breakage of the Cr coating corresponds to the initial failure that can be seen at a load of 145 N [Fig. 8(a1)]. Here, elements such as Cr, aluminum, and titanium diffuse in the fabrication and oxidization process. When the Cr coatings are fabricated by using the surface alloying technology, the argon ions at a concentration of $10^{17}/cm^2$ bombard the surface of substrate.[18] Thus, a high-concentration vacancy defect layer forms, where the defects

are distributed in a gradient manner. These high-concentration vacancy defects play a key role in the diffused layer, leading to a strong adhesion force. Therefore, the critical load at the first spall is larger for the Cr-coated specimen than other results,[15,27,28] Numerous fine cracks on the order of ~ 2 μm–3 μm can be seen on the scratching surface [Fig. 8(a1)]. However, the brittle oxide layers, such as Cr_2O_3, Al_2O_3, and TiO_2, form during being oxidized. The critical load split into two parts: a low load where an initial failure is initiated, named L_{c1}, and the other load corresponding to peeling off the coating, called L_{c2}. After the layer is oxidized for 90 h, the value of L_1 and L_2 are of 103 N and 106 N, respectively. When the oxidation time increases to 300 h, the L_1 and L_2 values decrease to 59 N and 65 N, respectively. The scratching surface of the coated substrates is full of microcracks after being oxidized for 90 h and 300 h [Figs. 8(b2)–8(c2)]. By comparison, the value of L_1 and L_2 of the uncoated Ti-45Al-8.5Nb specimen are 10 N and 21 N after being oxidized for 300 h, respectively.

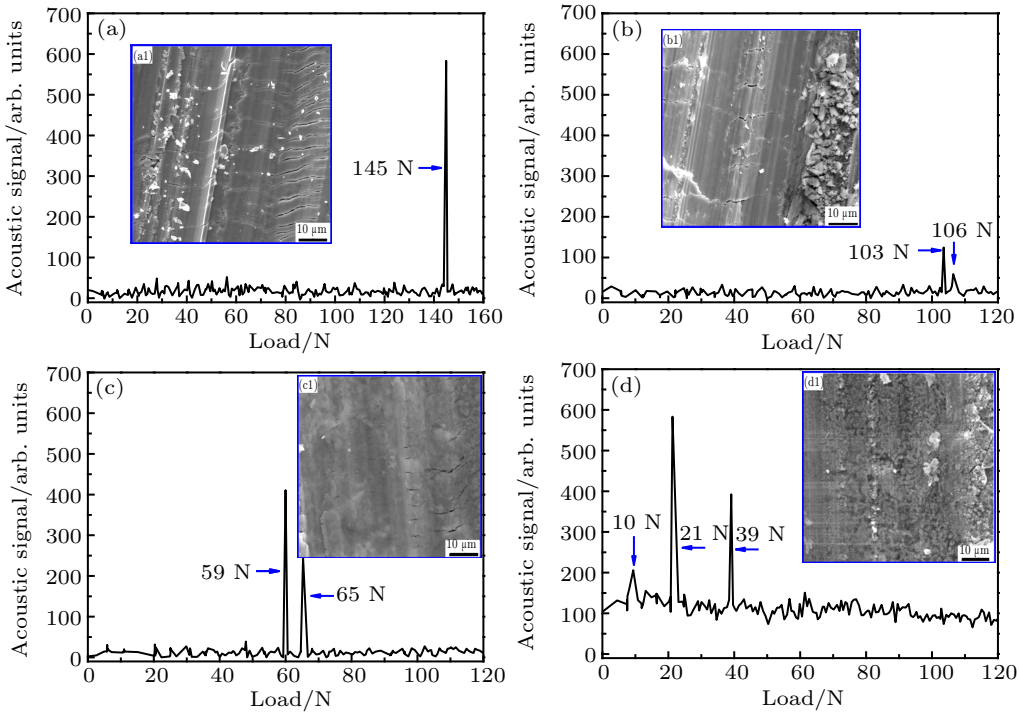


Fig. 8. Results of scratch tests on Cr/substrate fabricated at 1000 °C and oxidized for (a) 0 h with (a1) inset showing scratch morphology, (b) 90 h with (b1) inset showing scratch morphology, (c) 300 h with (c1) inset showing scratch morphology, and (d) 300 h with (a1) inset showing scratch morphology.

4. Discussion

The formation of oxides, including Al_2O_3, TiO_2, and Cr_2O_3 on the surface of specimen during oxidation, relates to the thermodynamics of their reactions.[25,29] Here, the formation free energy of Al_2O_3, TiO_2, and Cr_2O_3 are calculated, according to the free-energy-of-oxides standards presented by Ellingham, to be -795.72 kJ/mol, -662.84 kJ/mol, and -523.78 kJ/mol, respectively. Although the standard Gibbs free energy of formation of Al_2O_3 and TiO_2 are both lower than that of Cr_2O_3, the oxygen in air first contacts the Cr coating to form Cr_2O_3 due to the Cr-coated surface of the substrate. Yet, not all of the Cr coating is oxidized simultaneously on the surface during the initial oxidation. Oxygen atoms diffuse along the Cr grain boundary during the initial oxidation, which should combine with aluminum and titanium atoms to form Al_2O_3 and TiO_2 before a compact Cr_2O_3 film is formed (Fig. 2). Therefore, the Cr_2O_3, Al_2O_3, and TiO_2 phases are found in our XRD results after being oxidized for 1 h, 3 h, and 5 h (Fig. 3). However, the oxide films and Cr coating are so thin that the Ti_3Al and TiAl phases of the substrate can also be seen in our XRD results. Additionally, the diffraction intensity of the Cr_2O_3 phase gradually becomes stronger with initial oxidation time increasing.

In the isothermal oxidation process, increasing the number of Cr atoms in the coating can lead the Cr_2O_3 to form, and thus making the Cr_2O_3 film denser and further preventing the substrate to be oxidized. The distribution of oxygen atoms is consistent with the distribution of Cr atoms, corresponding to the oxide layers (Fig. 7). Comparing with the as-prepared Cr-coated substrates [see Figs. 1(c) and 1(f)], the thickness values of oxide layers for both specimens fabricated at 800 °C and 1000 °C are not obviously different after being oxidized for 90 h [see Figs. 7(c1) and 7(e1)]. This indicates that Cr atoms diffuse slightly in the oxidation process.

The oxygen atoms are distributed in three layers, they being the outermost layer with the highest concentration, the intermediate layer, and the inner layer [see Fig. 8(c2)]. However,

others, especially Cr atoms are distributed in two layers within the outermost and the inner layers [see Fig. 8(c6)]. This suggests that a Cr_2O_3 film forms in the outermost layer, but Cr and oxides including Cr_2O_3, Al_2O_3, and TiO_2 co-exist in the intermediate layer [see Figs. 4 and 7(c)],resulting in a high adhesion force, such as an L_1 up to 103 N [Fig. 9(b)]. By comparison, after being oxidized for 300 h [see Figs. 6 and 7(d1)], the compact Cr_2O_3 film grew towards the outside, with a thickness over ~6 μm (deposition at 800 °C) and ~ 10 μm (deposition at 1000 °C). Due to the formation of the thick Cr_2O_3 film, oxygen diffusion slows down. Thus, the oxidation weight rate decreases [see Fig. 5(b)]. The adhesion force drops to ~ 60 N [see Fig. 9(c)], which is still higher than the value of uncoated Ti-45Al-8.5Nb specimen after being oxidized for 300 h.

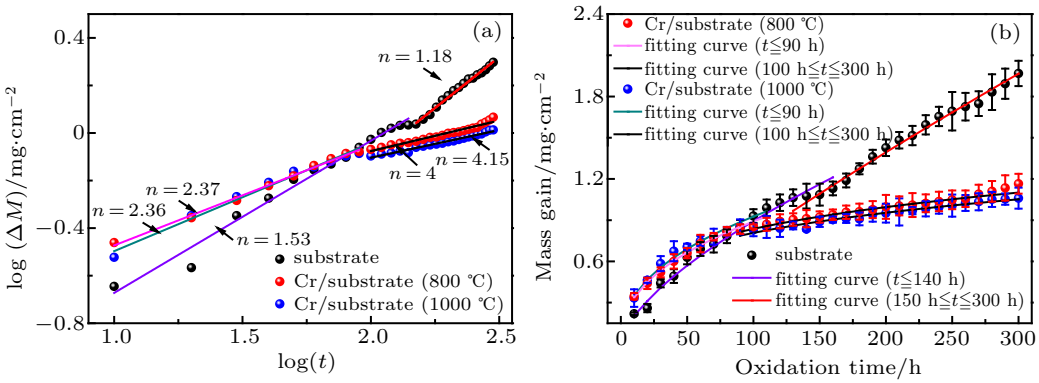


Fig. 9. Isothermal oxidation kinetic (a) log–log curves and (b) fitting curves.

Table 4. Kinetic parameters of Isothermal oxidation.

Sample	n	k/mg^n·cm^{-n}·h^{-1}	Equation	Time/h
Substrate	1.67 ± 0.1	0.0088	$(\Delta M)^{1.67} = 8.8 \times 10^{-3} t$	≦ 140
Substrate	1.18±0.65	0.0074	$(\Delta M)^{1.18} = 7.4 \times 10^{-3} t$	≧ 150
Cr/S. (800 °C)	$1.96 + 0.14$	0.0085	$(\Delta M)^{1.96} = 8.5 \times 10^{-3} t$	≦ 90
Cr/S. (800 °C)	$3.92 + 0.09$	0.0049	$(\Delta M)^{3.92} = 4.9 \times 10^{-3} t$	≧ 100
Cr/S. (1000 °C)	$2.08 + 0.05$	0.0088	$(\Delta M)^{2.08} = 8.8 \times 10^{-3} t$	≦ 90
Cr/S. (1000 °C)	$4.1 + 0.12$	0.0041	$(\Delta M)^{4.1} = 4.1 \times 10^{-3} t$	≧ 100

According to Wagner's theory,[29] the weight gain can be determined as follows:

$$\Delta M^n = k_n t, \tag{1}$$

where ΔM is the weight gain of per unit area (in units mg/cm^2), n is the oxidation exponent, k_n is a constant of the oxidation reaction rate, and t is the oxidation time (in unit h). By fitting our isothermal oxidation results [Fig. 9(a)], the oxidation process can be divided roughly into two stages [Fig. 9(b)]. The n and k_n are calculated and the results are in Table 4. For an uncoated Ti-45Al-8.5Nb specimen, the oxidation exponent is ~ 1.7 within ~ 140 h but drops to ~ 1.2 (a linear relation) after 140 h. It is believed that the continuous Al_2O_3 film is hardly formed due to the competitive growth between TiO_2 and Al_2O_3, leading to the weak oxidation resistance.[2–5] However, for the Cr-coated specimen, its power exponent is ~ 2.0 at the first ~ 90 h of oxidation. This nearly parabolic reaction rate indicates that the continuous oxide film gradually thickens with oxidation time increasing, but the oxidation weight gain rate decreases. The power exponent of the Cr-coated alloy increases to ~ 4 between ~ 90 h and 300 h, suggesting that a protective oxide film forms on the substrate surface, which can prevent the substrate surface from being oxidized.

In addition, the element inter diffusion plays an important role in the integrity property of coatings such as phase stability, microstructure and adhesion. Here, elements such as Cr, Al, and Ti will diffuse in the fabricating and oxidizing process. The related parts of main elements are chosen from the as-prepared specimens of Figs. 1(c) and 1(f), and from the specimens after being oxidized as done in Figs. 6(a2)–6(d2). Due to the non-steady diffusion, the Fick's second law is employed to describe the diffusion behaviors of atoms:[25]

$$\frac{\partial C}{\partial t} = D \frac{\partial^2 C}{\partial x^2}, \tag{2}$$

where C is the concentration of any diffusing locations, D is the diffusion coefficient, t is the diffusion time, and x is the diffusion location. The relationship among the concentration, diffusion time, and location can be obtained by using a solution based on Gaussian function

$$C(x,t) = \frac{2M}{\sqrt{\pi D t}} \exp\left(\frac{-(x-x_0)^2}{4Dt}\right), \tag{3}$$

where M is the initial concentration of the diffusion boundary, x_0 is the location of diffusion boundary. Here, for as-prepared

specimens, their values of D of Cr atom are 4.40×10^{-4} μm^2/s and 7.54×10^{-4} μm^2/s, respectively, which are higher than the values of D of Al and Ti (Table 5). By comparison, the values of D of corresponding elements after being oxidized are lower than those of as-prepared specimens. For instance, the value of D of Cr atom after 90-h oxidation is 7.55×10^{-7} μm^2/s. The D values of current results are larger than the Tsai's conventional diffusion results.[30] Usually, an intrinsic vacancy defects' concentration exists in the substrate at a given temperature. However, during the Cr-coatings being fabricated by the surface alloying technology, the argon ions with a concentration of 10^{17}/cm^2 bombard the substrate surface.[18] So, a high-concentration vacancy defect layer is created, where the defects distributed in a gradient manner. These high-concentration vacancy defects play a key role in the diffusion layer, leading to a strong adhesion force.

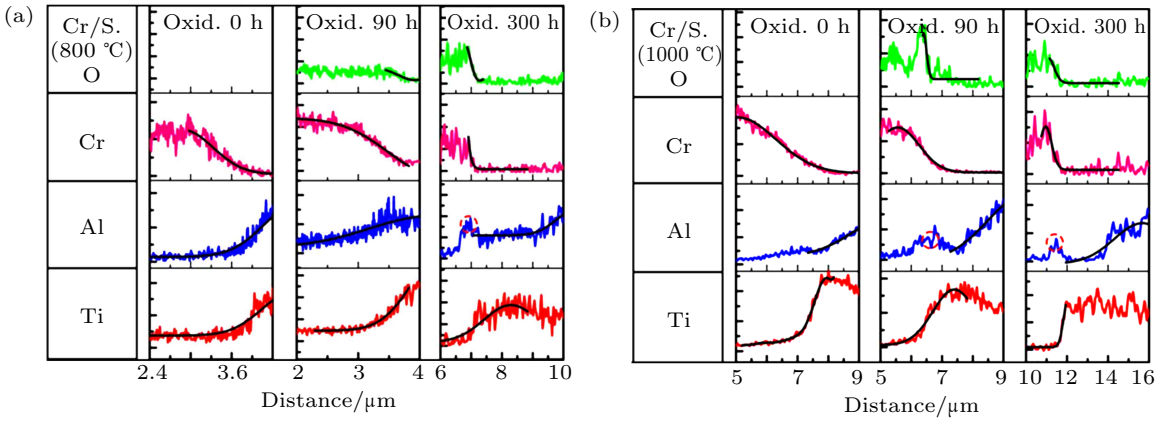


Fig. 10. EDS line-scan profiles of Cr/substrate fabricated at (a) 800 °C marked in Figs. 1(c), 6(a2), and 6(b2). (b) 1000 °C marked in Figs. 1(e), 6(c2), and 6(d2).

Table 5. Diffusion coefficients before and after Cr/substrate has been oxidized (in units of μm^2·s^{-1}).

Sample	Cr/S. (800 °C) D/μm^2·s^{-1}	Cr/S. (1000 °C) D/μm^2·s^{-1}	Cr/S. (800 °C) Oxid. 90 h D/μm^2·s^{-1}	Cr/S. (1000 °C) Oxid. 300 h D/μm^2·s^{-1}	Cr/S. (800 °C) Oxid. 90 h D/μm^2·s^{-1}	Cr/S. (1000 °C) Oxid. 300 h D/μm^2·s^{-1}
O Kal	–	–	1.03×10^{-7}	7.67×10^{-8}	1.87×10^{-8}	4.32×10^{-8}
Cr Kal	7.54×10^{-4}	4.40×10^{-4}	8.56×10^{-7}	7.55×10^{-7}	6.73×10^{-8}	3.96×10^{-8}
Al Kal	6.59×10^{-5}	6.85×10^{-5}	1.57×10^{-6}	2.4×10^{-6}	1.78×10^{-7}	8.93×10^{-7}
Ti Kal	5.69×10^{-5}	8.19×10^{-5}	4.47×10^{-7}	7.49×10^{-7}	3.57×10^{-7}	2.02×10^{-8}
Nb Kal	6.76×10^{-5}	5.21×10^{-4}	8.56×10^{-7}	4.81×10^{-6}	1.8×10^{-7}	4.6×10^{-8}

In short, the Cr_2O_3 as the oxidation resistance layer forms due to the deposited Cr coating during isothermal oxidation. The diffused Cr layer during fabrication plays a vital role in implementing the good adhesion between the coating and substrate. Therefore, the anti-oxidation and the adhesion of Cr-coated Ti-45Al-8.5Nb alloy are improved via PSMT.

5. Conclusions

The dense, crack-free Cr coatings including a deposited and diffused layer are fabricated on a Ti-45Al-8.5Nb substrate by PSAT at 800 °C and 1000 °C, respectively. The Cr-coated specimens each exhibit good adhesion. Oxides, including Cr_2O_3, Al_2O_3, and TiO_2, are simultaneously found by XRD pattern after initially being oxidized at 900 °C. The Cr_2O_3 covers the surface after being isothermally oxidized, *e.g.*, for 300 h. The oxidation kinetic curves of the Cr-coated specimens can are roughly be divided two stages according to the weight gaining rate, which cab be described by a stage with a parabolic law, and a biquadratic law stage. The adhesion force of Cr-coated specimen is 59 N after being oxidize for 300 h, which is higher than that of uncoated specimen. Thus, the Cr-coated Ti-45Al-8.5Nb alloy achieves a good oxidation protection.

References

[1] Yamaguchi M, Inui H and Ito K 2000 *Acta Mater.* **48** 307
[2] Kim Y W 1989 *JOM* **41** 24
[3] Becker S, Rahmel A, Schorr M and Schütze M 1992 *Oxid. Metal.* **38** 425
[4] Yoshihara M and Kim Y W 2005 *Intermetallics* **13** 952
[5] Lin J P, Zhao L L, Li G Y, Zhang L Q, Song X P, Ye F and Chen G L 2011 *Intermetallics* **19** 131
[6] Zhang X J, Li Q, Zhao S Y, Gao C X, Wang L and Zhang J 2008 *Appl. Surf. Sci.* **255** 1860
[7] Cheng Y X, Wang W, Zhu S L and Wang F H 2009 *Corros. Sci. Prot.* **21** 266
[8] Taniguchi S, Shibata T and Murakamit A 1994 *Oxid. Metal.* **41** 103
[9] Wei XF, Zhang PZ, Wei D B, Zhou P, Zhang Y, Chen XH, Wang Q and Wang R N 2014 *Rare Met. Mater. Eng.* **43** 707
[10] Ren B, Miao Q, Liang W P, Wang L, Xia J J and Liu W 2015 *Corros. Sci. Prot.* **27** 363
[11] Braun R, Fröhlich M and Leyens C 2010 *Int. J. Mater. Res.* **101** 637

[12] Kim D J, Seo D Y, Huang X, Yang Q and Kim Y W 2012 *Surf. Coat. Technol.* **206** 3048
[13] Chen R R, Gong X, Wang Y, Qin G, Zhang N N, Su Y Q, Ding H S, Guo J J and Fu H Z 2018 *Corros. Sci.* **136** 244
[14] Yao J Q, He Y D, Wang D R and Lin J P 2014 *Corros. Sci.* **80** 9
[15] Yang X, Jiang Z P, Hao G J, Liang Y F, Dong X F and Lin J P 2018 *Appl. Surf. Sci.* **455** 144
[16] Anghel E M, Marcu M, Banu A, Atkinson I, Paraschiv A and Petrescu S 2016 *Ceram. Int.* **42** 12148
[17] Xu Z, Liu X, Zhang P, Zhang Y, Zhang G and He Z 2007 *Surf. Coat. Technol.* **201** 4822
[18] Xu Z and Xiong Frank F 2017 *Plasma surface metallurgy with double glow discharge technology-Xe-tec process* (Beijing: Science Press)
[19] Wei D B, Chen X H, Zhang P Z, Ding F, Li F K and Yao Z J 2018 *Appl. Surf. Sci.* **441** 448
[20] Zhang X, Xie X S, Yang Z M, Dong J X, Xu Z, Gao Y and Zhang T H 2000 *Surf. Coat. Tech.* **131** 378
[21] Qin L, Yang K K, Liu C S and Tang B 2012 *Mater. Lett.* **82** 127
[22] Wei D B, Zhang P Z, Yao Z J, Liang W P, Miao Q and Xu Z 2013 *Corros. Sci.* **66** 43
[23] Wei D B, Zhang P Z, Yao Z J, Zhou J T, Wei X F and Zhou P 2012 *Appl. Surf. Sci.* **261** 800
[24] Chen X H, Zhang P Z, Wei D B, Ding F, Li F K, Wei X F and Ma S J 2018 *Mater. Lett.* **215** 292
[25] Paul A, Lauril T, Vuorinen V and Divinski S V 2014 *Thermodynamics, Diffusion and the Kirkendall Effect in Solids* (Springer Cham)
[26] Zhao L L 2010 *The high temperature oxidation behavior of high Nb containing TiAl alloys and effects of alloying elements* (Beijing: University of Science and Technology Beijing)
[27] Li XJ, Cheng G A, Xue W B and Cheng Y J 2007 *J. Aero. Mater.* **27** 1
[28] Wang D R 2012 *Proceedings of the* 9*th National Surface Engineering Conference and the* 4*th National Youth Surface Engineering Forum*
[29] Li M S 2001 *High temperature oxidation of metals* (Beijing: Metallurgical Industry Press)
[30] Tsai S C, Huntz A M and Dolin C 1996 *Mater. Sci. Eng. A* **212** 6